CSIRO PUBLISHING

Invertebrate Systematics, 2017, **31**, 233–248
http://dx.doi.org/10.1071/IS16078

eadem figura manet: Measuring morphological convergence in diplocentrid scorpions (Arachnida : Scorpiones : Diplocentridae) under a multilocus phylogenetic framework

Carlos E. Santibáñez-López[A,C,D], *Ricardo Kriebel*[B,C] *and Prashant P. Sharma*[A]

[A]Department of Zoology, University of Wisconsin – Madison, 430 Lincoln Drive, Madison, WI 53706, USA.
[B]Department of Botany, University of Wisconsin – Madison, 430 Lincoln Drive, Madison, WI 53706, USA.
[C]Authors contributed equally to this work.
[D]Corresponding author. Email: santibanezlo@wisc.edu

Abstract. Morphology still plays a key role in the systematics and phylogenetics of most of the scorpion families and genera, including the Diplocentridae Karsch, 1880. The monophyly of this family, and the monophyly of its two subfamilies is supported by morphological characters; however, neither hypothesis has been tested using molecular data. The lack of a molecular phylogeny has prevented the study of the evolution of morphology within the family. Here, we examine the morphological evolution of several key character systems in diplocentrid systematics. We tested the monophyly of the Diplocentridae, and subsequently the validity of its two subfamilies using a five-locus phylogeny. We examined the variation and evolution of the shape of the carapace, the external surface of the pedipalp patella and the retrolateral surface of the pedipalp chelae of males and females. We also examined the phylogenetic signal of discrete and continuous characters previously reported. We show that Diplocentridae is monophyletic, but Nebinae is nested within Diplocentrinae. Therefore, Nebinae is synonymised with Diplocentrinae (**new synonymy**). Finally, we show that a new character system proposed here, tarsal spiniform and macrosetal counts, retains high phylogenetic signal and circumscribes independently evolving substructures within this character system.

Additional keywords: comparative methods, dated phylogeny, phylogenetic signal, trait correlation.

Received 19 November 2016, accepted 15 January 2017, published online 2 May 2017

Introduction

Until recently, morphology was the only source of information in the systematics and phylogenetics of scorpion families and genera (e.g. Prendini 2000, 2003; Francke and Prendini 2008; Prendini *et al*. 2010; Prendini and Esposito 2010; Francke *et al*. 2014; Monod and Prendini 2015). However, more recent studies have included molecular sequence data (e.g. Prendini *et al*. 2003; Santibáñez-López *et al*. 2014*a*; González-Santillán and Prendini 2015; Ojanguren-Affilastro *et al*. 2016) and have implemented parametric approaches to phylogenetic inference. A recent phylogenomic analysis of the entire order (Sharma *et al*. 2015) revealed discordance with the historical morphological relationships (Coddington *et al*. 2004), suggesting that homoplasy and morphological convergence are present in morphological matrices at higher taxonomic levels. However, that phylogenomic study sampled only 25 ingroup taxa (1–4 exemplars per family), and intrafamilial relationships were not explored. Inversely, González-Santillán and Prendini (2015) showed that discrete morphological characters for the vaejovid subfamily Syntropinae have high consistency and retention indices, whereas meristic characters were less informative. It is therefore not clear whether different morphological character systems are also homoplastic within scorpion families and genera, and whether reliable (traditional) character systems can be identified towards resolving the systematics of genera and species groups.

To our knowledge, molecular phylogenetic analyses of only two scorpion families have been published to date (Fet *et al*. 2003; Prendini *et al*. 2003; see also González-Santillán and Prendini 2015 for a thorough analysis of the subfamily Syntropinae) and two unpublished works have been presented at international meetings (Prendini and Wheeler 2004; Mattoni *et al*. 2010). Whereas in the first published analysis, Fet *et al*. (2003) used only one locus (*16S* rRNA) to revise the phylogenetic relationships of exemplar species of Buthidae, the second analysis included four molecular regions of two loci to explore the relationships between scorpionid genera (Prendini *et al*. 2003). However, both analysed their datasets using cladistic methods, and neither assessed homoplasy and morphological convergence within Buthidae or Scorpionidae, respectively.

An ideal system for the examination of the evolution of morphology at the family level in scorpions is Diplocentridae. This family currently comprises two subfamilies: Nebinae

Kraepelin, 1950, with only one genus and nine species, and Diplocentrinae Karsch, 1880, with nine genera and ~120 species. Scorpions of this family range in size from small (adults of *Diplocentrus bereai* (Armas & Martín-Frías, 2004) and *Oiclus purvesii* (Becker, 1880) ranging from 20 to 30 mm) to larger species (adults of *D. taibeli* (Caporiacco, 1938), *Kolotl magnus* (Beutelspacher & López-Forment, 1991) and *Nebo hierichonticus* (Simon, 1872) ranging from 80 to 90 mm). Almost all species within this family are fossorial, although two *Diplocentrus* inhabit caves: the strictly troglobitic (i.e. lacking eyes and pigmentation) *D. anophthalmus* Francke, 1977, and the troglophilic *D. cueva* Francke, 1978, which has reduced eyes and elongated appendages (but see also Volschenk and Prendini 2008). These scorpions exhibit morphological variation, especially in the pedipalp morphosculpture (i.e. pedipalp carination: Santibáñez-López *et al.* 2014*a*,*b*), although some other characters might also be homoplastic (e.g. carapace morphology, number of telotarsal and basitarsal spiniform macrosetae).

The monophyly of Diplocentridae (*sensu* Prendini 2000) is supported by three characters: a fused lamellar hook and median lobe of the hemispermatophore, the presence of the subaculear tubercle, and the red venom coloration. While the monophyly of Diplocentrinae is supported by three characters – the laterodistal lobes of telotarsi rounded (truncated in Nebinae), the development of the carination on metasomal segments III and IV, and the transverse carina on metasomal segment V – the monophyly of Nebinae is supported by only one character (the position of trichobotrium *it* distal to *ib*). However, within Diplocentrinae, the internal relationships were not fully resolved, and some genera were recovered as paraphyletic (e.g. *Diplocentrus*) (Prendini 2000). As suggested by Prendini (2000), this result relies on the fact that most of the diplocentrine genera are diagnosed by morphometric data (e.g. *Cazierus*, *Oiclus*, *Didymocentrus*). Thus, Prendini (2000) concluded that the inclusion of molecular data would provide a better framework to resolve the relationships within this group.

Recently, Santibáñez-López *et al.* (2014*a*) provided a multilocus phylogenetic analysis of *Diplocentrus* based on exemplar taxa, covering the entire geographical distribution and morphological diversity in the genus. This analysis included the type species of *Didymocentrus*, *Bioculus* and *Tarsoporosus* to assess the generic limits of *Diplocentrus*. However, these authors did not test the monophyly of the subfamily, because the tree was rooted with *Heteronebo jamaicae* Francke, 1978, a Caribbean diplocentrid.

To understand morphological evolution in what appears to be a morphologically 'homogeneous' scorpion family, a multilocus phylogeny of Diplocentridae was inferred in this study. The traditional discrete, as well as meristic, characters were examined to measure phylogenetic signal, character correlation, and the influence of sexual dimorphism on diagnostic characters (such as the shape of the pedipalp chela). Concomitantly, the systematic utility of diplocentrid taxonomic ranks in the context of the molecular phylogeny, and the phylogenetic signal of discrete and meristic characters, were evaluated. Finally, for the first time, a dated molecular phylogeny was estimated for the group.

Materials and methods

Molecular sequence data

The complete five-locus dataset used in Santibáñez-López *et al.* (2014*a*) was retrieved from GenBank. Following the phylogenomic relationships recovered by Sharma *et al.* (2015), we selected the following species as outgroups: two scorpionids (*Pandinus imperator* (C.L. Koch, 1841) and *Heterometrus fulvipes* (C.L. Koch, 1837)), two hormurids (*Opisthacanthus madagascariensis* Kraepelin, 1894 and *Liocheles australasiae* (Fabricius, 1775)), one urodacid (*Urodacus planimanus* Pocock, 1893), one bothriurid (*Bothriurus flavidus* Kraepelin, 1911), one vaejovid (*Smeringurus grandis* (Williams, 1970)), and one buthid (*Androctonus australis* (Linnaeus, 1758)). *Nebo hierichonticus* was included to represent the subfamily Nebinae (the putative sister group to subfamily Diplocentrinae). The buthid, *A. australis*, was used to root all tree topologies.

Available sequences for the outgroups were retrieved from GenBank or from the transcriptomic dataset of Sharma *et al.* (2015) (e.g. *18S* and *28S* rRNA sequences). For four taxa of the transcriptomic database, mitochondrial markers were not available (Table S1, available as Supplementary material to this paper). Preliminary analyses of the gene trees were conducted under a maximum-likelihood framework (see below) to test for potential contaminations. As a result of this screening, the *12S* rRNA and cytochrome *c* oxidase subunit I (*COI*) sequences from *Diplocentrus zacatecanus* were removed because their placement suggested contamination, likely with a bothriurid species. The final dataset, with accession numbers, is provided in Table S1.

Imaging

Specimens of *Diplocentrus* were imaged in dorsal view of the carapace, dorsal retrolateral view of the pedipalp chela, and the retrolateral view of the pedipalp patella, when possible. Other images were taken from the available literature (e.g. Santibáñez-López *et al.* 2013*a*, 2013*b*). Photographs were taken using a Nikon SMZ-800 with a Nikon Coolpix S10 VR camera attachment. Modal tarsal spiniform formulae were recovered from adults from all diplocentrid terminals. Composite schematics of the tarsal segments of legs I–III combining information from *Bioculus caboensis* (Stahnke, 1968), *Didymocentrus lesueurii* (Gervais, 1844), *Diplocentrus mexicanus* Peters, 1861, *D. keyserlingii* Karsch, 1880, *Heteronebo jamaicae*, *Kolotl poncei* (Francke & Quijano-Ravell, 2009), *Nebo hierichonticus*, and *Tarsoporosus kugleri* (Schenkel, 1932) were generated using Adobe Illustrator CS6 from drawings of adult females or males under a Nikon SMZ-800 microscope.

Phylogenetic reconstruction

Multiple sequence alignments for each of the five gene fragments (*12S* rRNA, *16S* rRNA, *18S* rRNA, *28S* rRNA and *COI*) were generated using MUSCLE 3.8.31 (Edgar 2004), and ambiguously aligned regions were culled with GBlocks 0.91b (Castresana 2000), resulting in a matrix consisting of 46 terminals and 4126 bp. Maximum-likelihood (ML) analysis was conducted in RAxML 8.2.4 (Stamatakis 2014) employing a GTR + Γ model (for each partition) with 500 independent starts and 1000 bootstrap replicates. The Bayesian inference (BI)

analysis was performed using MrBayes 3.2.2 (Ronquist *et al.* 2012) using a GTR + Γ + I model for each partition under the Akaike information criterion (as explained in Posada and Buckley 2004) selected in jModelltest 2 (Guindon and Gascuel 2003; Darriba *et al.* 2012). Four runs each with four Markov chains (default distribution of chain temperatures) were implemented for 2×10^7 generations using default priors and discarding 5×10^6 generations (25%) as burnin.

A dated molecular phylogeny was estimated using BEAST 1.8.3 (Drummond *et al.* 2012) with a unique GTR + Γ + I model for each partition. *COI* was partitioned with two separate site models, for first and second positions versus the third codon position. A birth–death model was used for the tree prior, and an uncorrelated relaxed clock (Drummond *et al.* 2006) with a log-normal distribution was implemented for each partition. Since no diplocentrid or scorpionid fossils are known for use as calibration priors, the root age was constrained using a normal distribution with mean 381 million years and standard deviation of 23, based on the phylogenomic dating in this study (Sharma, unpublished data). Five independent runs consisting of 5×10^7 generations were computed, 1×10^7 generations (20%) were discarded as burn-in, with convergence assessed using Tracer 1.6 (Rambaut *et al.* 2014).

Multivariate analysis of shape data

To calculate morphological shape variation, the geometric morphometric technique of elliptic Fourier analysis (EFA) with the R package Momocs (Bonhomme *et al.* 2014) was applied. Outlines were extracted from images using GIMP 2.8 (http://www.gimp.org) and converted into monochromatic.jpeg files. Four structures were imaged: (1) male carapace, dorsal view, (2) male pedipalp patella, retrolateral view, (3) male pedipalp chela, dorsal retrolateral view, and (4) female pedipalp chela, dorsal retrolateral view. These structures were selected because of their historical utility for distinguishing groups in the Diplocentridae. A separate family of analyses was conducted for the complete dataset (all specimens available for the whole family), as well as the subset of *Diplocentrus* only.

Outlines were imported into R, converting them into lists of coordinates that describe the closed outlines. Their proper alignment was checked and the number of harmonics necessary to retain 99.9% of harmonic power during the EFA was calculated using the calibrate_harmonicpower function in Momocs. For all structures, 25 harmonics were enough to achieve this amount of power, and thus this number was used in the EFA. Additional arguments for the EFA included the normalisation of coefficients, and a single smoothing iteration. The resulting coefficients were then summarised using Principal Component Analysis (PCA) and the principal components (PCs) used to visualise the variation in morphospace. The number of PCs analysed was limited to those that explained 80% of variance in the dataset. These PCs were also matched to the phylogeny of Diplocentridae for downstream analyses.

The dated molecular phylogeny from BEAST was culled to retain only the intersection of terminals with available shape data. This intersection varied depending on the structure and data availability. Visualisation of morphospace as well as the change of shape through time using traitgrams were done with functions from Momocs and phytools (Revell 2012).

Analysis of sexual dimorphism

To characterise the evolution of sexually dimorphic characters pertinent to systematics, female and male pedipalp chelae were compared. After the EFA and PCA of the harmonic coefficients, multivariate analysis of variance (MANOVA) was used to compare shapes between sexes. Only species for which both female and male specimens were available were included in the MANOVA. Deformations between female and male chelae were determined using Thin Plate Splines with the tps_iso function in Momocs, and Euclidean distances were calculated between female and male chelae of all species using the truss function and providing the scores of the first three PCs. The resulting Euclidean distances represented our measurement of sexual dimorphism for visualising the variation of morphology through time.

Phylogenetic signal and trait correlation in discrete morphological characters

To test the stability of the phylogenetic topology using only morphological data, as previously reported in Santibáñez-López *et al.* (2014*a*), the 95 morphological characters were coded for *N. hierichonticus*, which served as outgroup to root the tree (representing the subfamily Nebinae). Parsimony analyses were conducted in TNT 1.5 (Goloboff *et al.* 2008) using the same strategy search used in Santibáñez-López *et al.* (2014*a*). To observe the differences between the topology recovered with the inclusion of *N. hierichonticus* and the topology presented in the previous study (Santibáñez-López *et al.* 2014*a*), Robinson–Foulds distances were calculated (Robinson and Foulds 1981). The selected topologies compared were those recovered with the analysis using implied weights and a *k* value of 100 (favoured because of their tree statistics). First, the tree topology recovered here was trimmed by removing *N. hierichonticus* so both trees contained the same taxa; then, the Robinson–Foulds distance was calculated with the phangorn package for R (Schliep 2011).

To measure the phylogenetic signal of the discrete morphological characters, the dated molecular phylogenetic tree was used as a reference topology (i.e. an independent data class) after culling outgroups, and a simple permutation test was conducted. The character histories of the 95 characters used in Santibáñez-López *et al.* (2014*a*) were reconstructed using parsimony ancestral states and likelihood ancestral states in Mesquite 3.10 (Maddison and Maddison 2016). Terminal taxa were reshuffled 1000 times, and parsimony character steps and the Mk1 substitution rates were recalculated on each replicate to generate a null distribution. From the resulting distribution of parsimony steps and Mk1 estimates, a *P* value was calculated, and significance was assessed at $\alpha = 0.05$ (one-tailed test). Characters with empirical parsimony steps or Mk1 substitution rates significantly less than their corresponding null distributions were taken as evolving non-randomly.

To test the independence of these selected characters, pairwise tests for correlation (binary characters only) were conducted with BayesTraits 2.0 (Pagel and Meade 2006) using the

discrete independent and discrete dependent models, and the Bayes factor comparisons for competing models.

Phylogenetic signal, trait correlation and variation in continuous characters

Quantitative characters are rarely used in scorpion phylogenetics (e.g. Prendini *et al.* 2003; González-Santillán and Prendini 2015) because of the difficulty in converting them to discrete characters, even when they are traditionally favoured in the literature (e.g. Francke 1977*a*, 1978, 1980). In the analysis of the subfamily Syntropinae (González-Santillán and Prendini 2015), quantitative characters used had a mean and a median of their consistency (CI) and retention (RI) indices below 0.5; however, the phylogenetic signal of these characters was not quantified under a model-based (non-parsimony) approach. In diplocentrid systematics, spiniform macrosetae counts in the telotarsi of walking legs are a reliable set of meristic characters to diagnose species (e.g. Francke 1977*b*; Santibáñez-López *et al.* 2013*a*, 2013*b*). Nevertheless, their phylogenetic signal in the evolution of dipocentrids has never been measured. Therefore, we selected 11 telotarsal and basitarsal modal counts from the 36 diplocentrid species studied here (Table S2).

To quantify phylogenetic signal of macrosetal counts, three indices were considered: Abouheif's C_{mean} (Abouheif 1999; Pavoine *et al.* 2008), Pagel's λ (Pagel 1999), and *K* of Blomberg *et al.* (2003). Abouheif's C_{mean} is an adaptation of the spatial autocorrelation to phylogenetic application, and quantifies the degree of correlation across observations, but without providing a model on trait origins (Vrancken *et al.* 2015). The latter two statistics pertain to a Brownian motion null model of trait evolution (Blomberg *et al.* 2003; Pagel and Meade 2006; Münkemüller *et al.* 2012). All indices were estimated with the Phylosignal package for R (Keck *et al.* 2016), using the dated molecular phylogeny recovered from BEAST 1.8.3 (after excluding outgroups, which could not be scored for these characters).

To test the independence or correlation of the continuous characters with phylogenetic signal, pairwise tests were also conducted using BayesTraits 2.0 under a random-walk model comparing two models (dependent and independent evolution), and evaluating the model with Bayes factor comparisons. Finally, the tarsal spiniform macrosetae counts were summarised in a PCA using the function dudi.pca of the ade4 library (Chessel *et al.* 2004) in R; the PCs were used to visualise variation across genera.

Results

Phylogeny and times of divergence of Diplocentridae

The BI, ML and BEAST phylogenetic analyses all recovered the monophyly of Diplocentridae (Fig. 1) with 94% bootstrap resampling frequency and maximal posterior probability values. However, the monophyly of Diplocentrinae was not recovered because of the nested position of *N. hierichonticus* in the BI and ML topologies as follows: ((*Di. krausi* + *Di. leusuerii*) (*N. hierichonticus* (*H. jamaicae* + *T. kugleri*))), albeit without high nodal support (Fig. 1); or as the sister group to *Didymocentrus* in the BEAST topology. The ML and BEAST topologies recovered *Kolotl*, *Bioculus* and *Diplocentrus* as monophyletic and their relationship as follows: (*Kolotl* (*Bioculus* + *Diplocentrus*)). The BI analysis did not recover the monophyly of *Diplocentrus* because of the exclusion of the '*zacatecanus*' group, albeit without nodal support, whereas the ML and BEAST analyses both recovered the monophyly of the three species groups within *Diplocentrus*, a result largely similar to the topology reported previously (Santibáñez-López *et al.* 2014*a*). However, the position of *Diplocentrus zacatecanus* within its species group was different from its previous placement, after the exclusion of two potentially contaminated sequences: (*D. silanesi* (*D. zacatecanus* (*D. whitei* + *D. peloncillensis*).

The estimation of divergence times under an uncorrelated relaxed clock model resulted in a dated phylogeny estimating the split between Diplocentridae and the rest of the non-buthid scorpions at 201 million years ago (Mya) (95% highest posterior density (HPD) interval: 133–246 million years (Ma)) (Fig. 2). Additionally, the split between *Bioculus* and *Diplocentrus* is estimated at 169 Mya (95% HPD interval: 110–236 Ma), with the most recent common ancestor of *Diplocentrus* inferred to be 158 Mya (95% HPD interval: 103–222 Ma). The diversification of the '*zacatecanus*' group was estimated at 66 Mya (median, 95% HPD interval: 40–99 Ma); whereas the '*mexicanus*' group split from the '*keyserlingii*' group 127 Mya (median, 95% HPD interval: 78–183 Ma). The estimated divergence of the '*keyserlingii*' group was recent (30 Mya, median, 95% HPD interval: 18–46 Ma), compared with the older '*mexicanus*' group (98 Mya, median, 95% HPD interval: 60–141 Ma).

Multivariate analysis of shape data

Carapace

In the EFA of the carapace across Diplocentridae, PC1 explained 56.3% of the variation, and shapes on this component range from a narrow to a broad carapace. PC2 explained 16.4% and varied in the degree of the development of the lateral lobes at the posterior margin of the carapace. PC3 explained 14.1% and varied in the shape of the carapace anterior median notch (from 'U' to 'V' shaped) (Fig. 3*A*). However, in the EFA of the carapace of only *Diplocentrus*, the morphospace showed considerable overlap between clades (Fig. S1*A*). The morphospace and phenogram of PC1 evidenced the unique morphology of *Diplocentrus anophthalmus* (the strict troglobite diplocentrid) of the '*mexicanus*' clade relative to the remaining Diplocentridae (Fig. 4*A*).

Male pedipalp patella

In the EFA of the retrolateral view of the pedipalp patella across all diplocenrids, PC1 explained 79.0% of the variation, and shapes on this component range from an overall slender to a wider patella. PC2 explained 11.2% and described the variation of the distal portion of the patella. PC3 explained 3.47% and described the variation related to the relative protrusion of the upper distal portion to the lower distal portion of the patella (Fig. 3*B*). There was no clear separation between the genera in the morphospace; *N. hierichonticus* is clustered with *K. poncei* and those *Diplocentrus* with slender patella on PC1. The shape of the patella of *Bioculus*, *Didymocentrus* and *Heteronebo* overlapped with some members of the '*keyserlingii*' group of *Diplocentrus*. In the analysis of *Diplocentrus*, the morphospace showed overlap

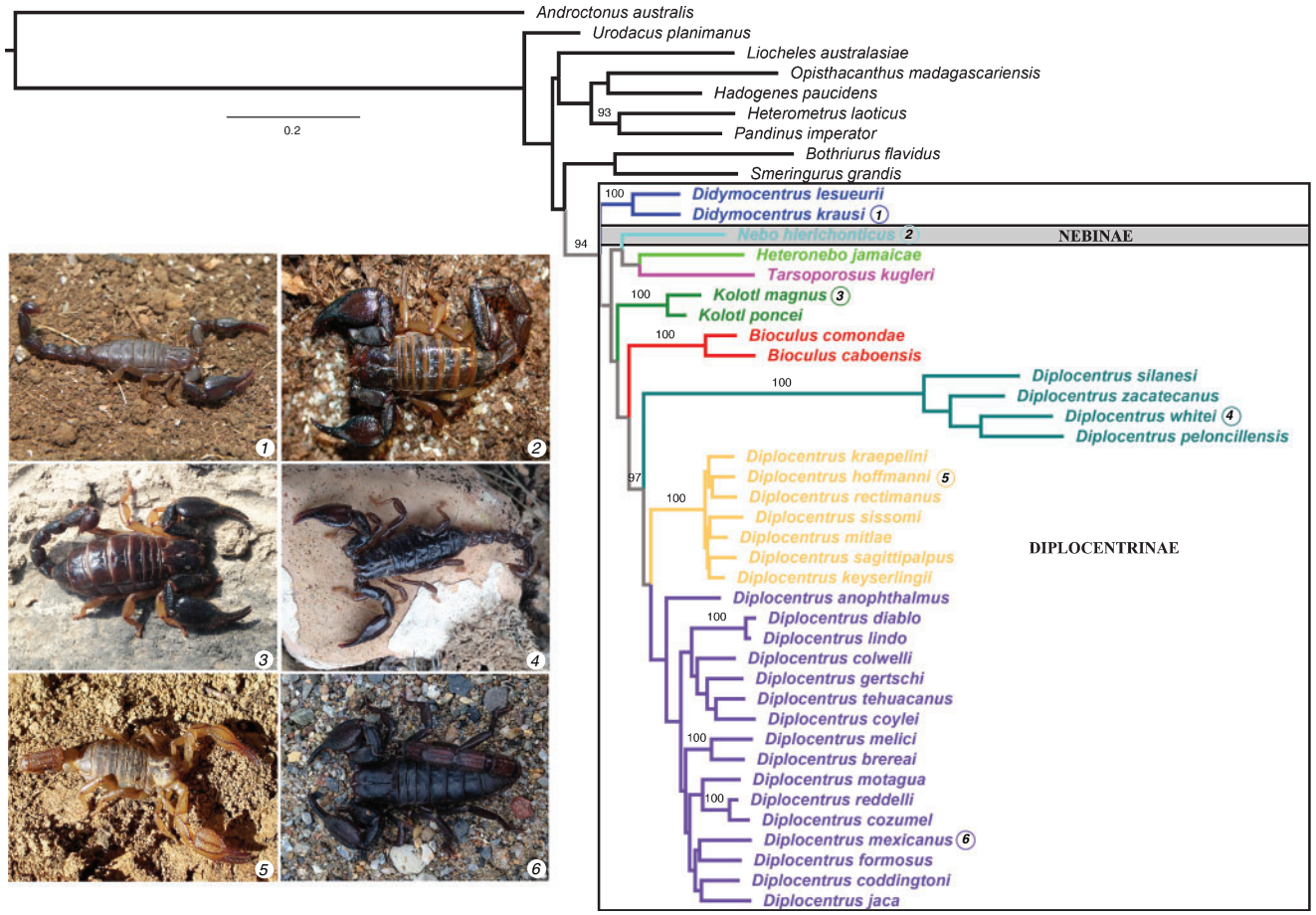

Fig. 1. Maximum-likelihood tree topology recovered from the analysis of five molecular markers, and 36 diplocentrid scorpion species plus nine outgroups (ln*L* = –29354.54). Colours in the tree are as follows: *Bioculus* (red), *Didymocentrus* (blue), *Heteronebo* (light green), *Kolotl* (green), *Nebo* (light blue), *Tarsoporosus* (pink). Within *Diplocentrus*: '*zacatecanus*' group (dark cyan), '*keyserlingii*' group (orange), and '*mexicanus*' group (purple). Bootstrap resampling frequencies >90% are indicated above branches. Left: Representatives of diplocentrid scorpion species: (*1*) adult female, *Didymocentrus* cf. *krausi* (photo by K. Sagastume); (*2*) adult male, *Nebo hierichonticus* (photo by J. Rein, The Scorpion Files©); (*3*) adult female, *Kolotl magnus*; (*4*) subadult female, *Diplocentrus whitei*; (*5*) adult male, *Diplocentrus hoffmanni*; (*6*) adult male, *Diplocentrus mexicanus*.

between the '*mexicanus*' and '*zacatecanus*' groups, which shared slender patellae. In contrast, the '*keyserlingii*' group showed some separation in the morphospace from the other two groups by the presence of a wider patella observed in several of its species (Fig. S1*B*). The phenogram of PC1 showed how the '*keyserlingii*' group diverged early on towards the wide shape spectrum of shape variation, and more recently it has converged with species of the other clades (Fig. 4*B*).

Female pedipalp chela

In the EFA of the female pedipalp chela of diplocentrids, PC1 explained 50% of the variation, and shapes on this component ranged from slender to rounded chelae, slender to wider fixed finger, and the degree of development of the dorsal lobe at the base of the manus. PC2 explained 21.1% and the variation in this PC corresponded to the curvature of the fixed finger, plus the height of the distal portion of the manus towards the fixed finger. Finally, PC3 explained 12.9%, describing the variation at the length of the fixed finger. All genera had largely similar female chela shape, except *N. hierichonticus*, which has the slenderest chelae of all (Fig. 3*C*). The phenogram of PC1 of female chela shape showed that most clades have stayed with a medium to broad shape, with a few instances of convergence to slender chelae in the '*keyserlingii*' and '*mexicanus*' groups (Fig. 4*C*, Fig. S1*C*).

Male pedipalp chela

In the EFA of the male pedipalp chela, PC1 explained 56.6% of the variation, and the shapes on this component ranged from slender to rounded chelae, short and wide to long and slender fixed fingers. PC2 explained 22.1% and the variation was shown on the length of the ventral margin from the base of the manus to the base of the movable finger articulation, and PC3 explained 8.94% and described the variation in the curvature of the fixed finger (from curved to straight). All genera had similar male chela shape except for *N. hierichonticus* and *D. silanesi*, which had the slenderest chela manus of all; however, the chela manus in *N. hierichonticus* is longer than

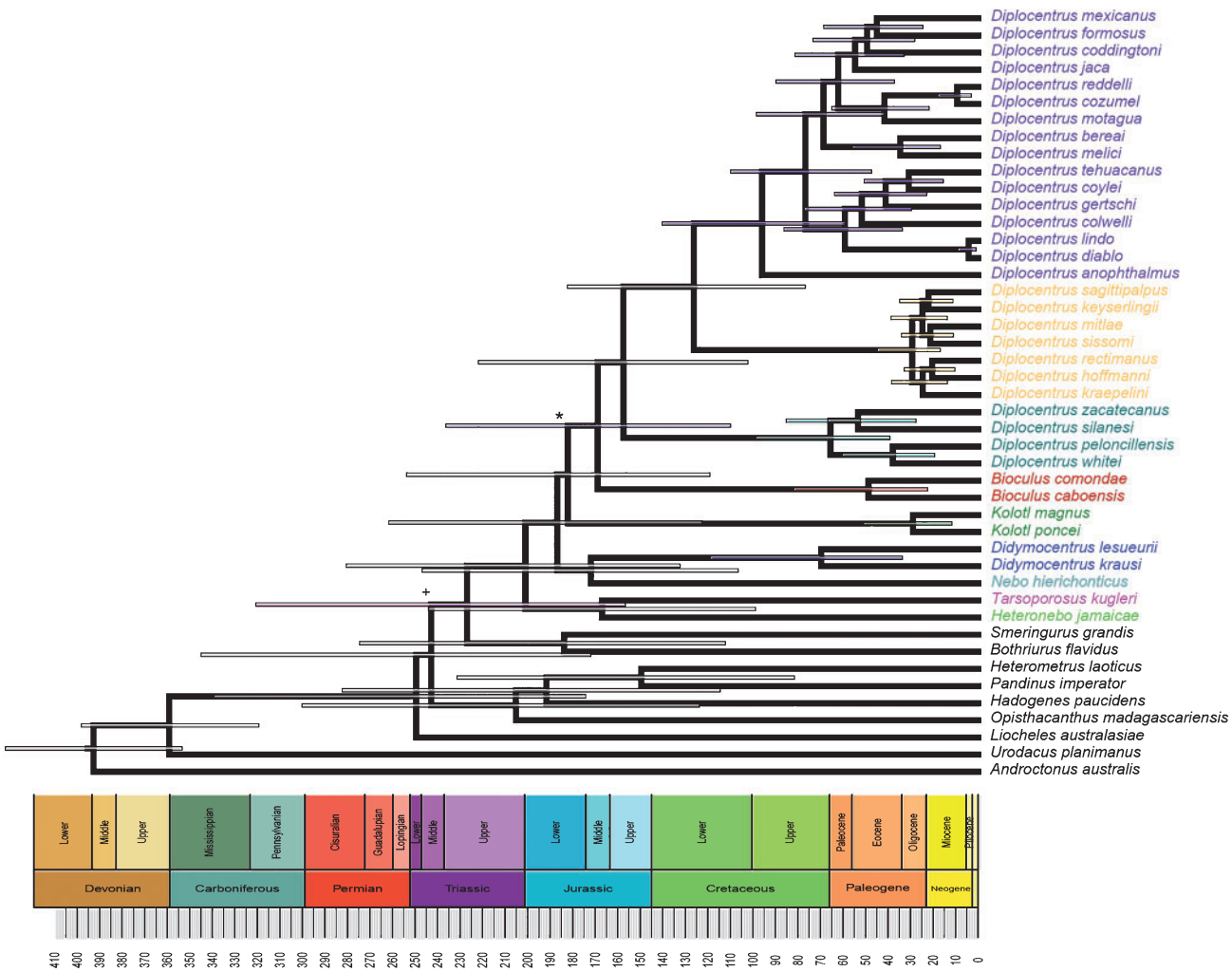

Fig. 2. Evolutionary tree with times of divergence inferred from the BEAST analysis of five molecular markers, and 36 diplocentrid scorpion species plus nine outgroups. Coloured bars correspond to the 95% HPD (highest probability density) intervals from the coloured names as follows: *Bioculus* (red), *Didymocentrus* (blue), *Heteronebo* (light green), *Kolotl* (green), *Nebo* (light blue), *Tarsoporosus* (pink). Within *Diplocentrus*: '*zacatecanus*' group (dark cyan), '*keyserlingii*' group (orange), and '*mexicanus*' group (purple). Cross indicates the origin of Diplocentridae; asterisk indicates the origin of *Diplocentrus*.

in *D. silanesi* (their separation in the PC1 versus PC2 in Fig. 3*D*). On the other hand, the chela manus of *Bioculus* and *Heteronebo* were the most rounded ones, with the shortest fingers of all. The morphospace as well as the phenogram of PC1 showed considerable overlap among genera, with convergence on the slenderest chelae on one end of the PC1 spectrum by *D. coddingtoni* and *D. silanesi*, and a distinctive pattern of evolution early on to the broadest chelae by *Bioculus* (Fig. 4*D*, Fig. S1*D*).

Sexual dimorphism in the pedipalp chela

Twenty-five diplocentrid species in the dataset had images available for both female and male pedipalp chelae. The MANOVA comparing the shape of female and male chelae showed a significant difference between both sexes ($F_{1,48} = 2.32$, $P = 0.02$). The Thin Iso Splines comparison of mean shape between the chelae of both sexes evidenced the strongest differences at two discontinuous parts of the podomere. First, the fixed finger of the female is curvier and shorter, whereas the fixed finger of the male chela is straighter and longer. Second, the female chela tends to have a more protruding lobe at the basal outer margin of the chela, whereas that of male does not (Fig. 5). The phenogram of sexual dimorphism showed that although most diplocentrid species do not show strong dimorphism, at least one species in each of the three clades of *Diplocentrus* has evolved strong (difference in Euclidean distance >0.06) sexual dimorphism, e.g. *D. reddelli* ('*mexicanus*' group), *D. zacatecanus* ('*zacatecanus*') and *D. mitlae* ('*keyserlingii*').

Phylogenetic signal in morphological characters

The parsimony analyses of the 36 diplocentrids (*N. hierichonticus* added; no outgroups) and 95 morphological characters were not congruent with the previously reported analysis of the same matrix, but without *N. hierichonticus* (Fig. 6). The inclusion of *N. hierichonticus* resulted in the paraphyly of *Diplocentrus*

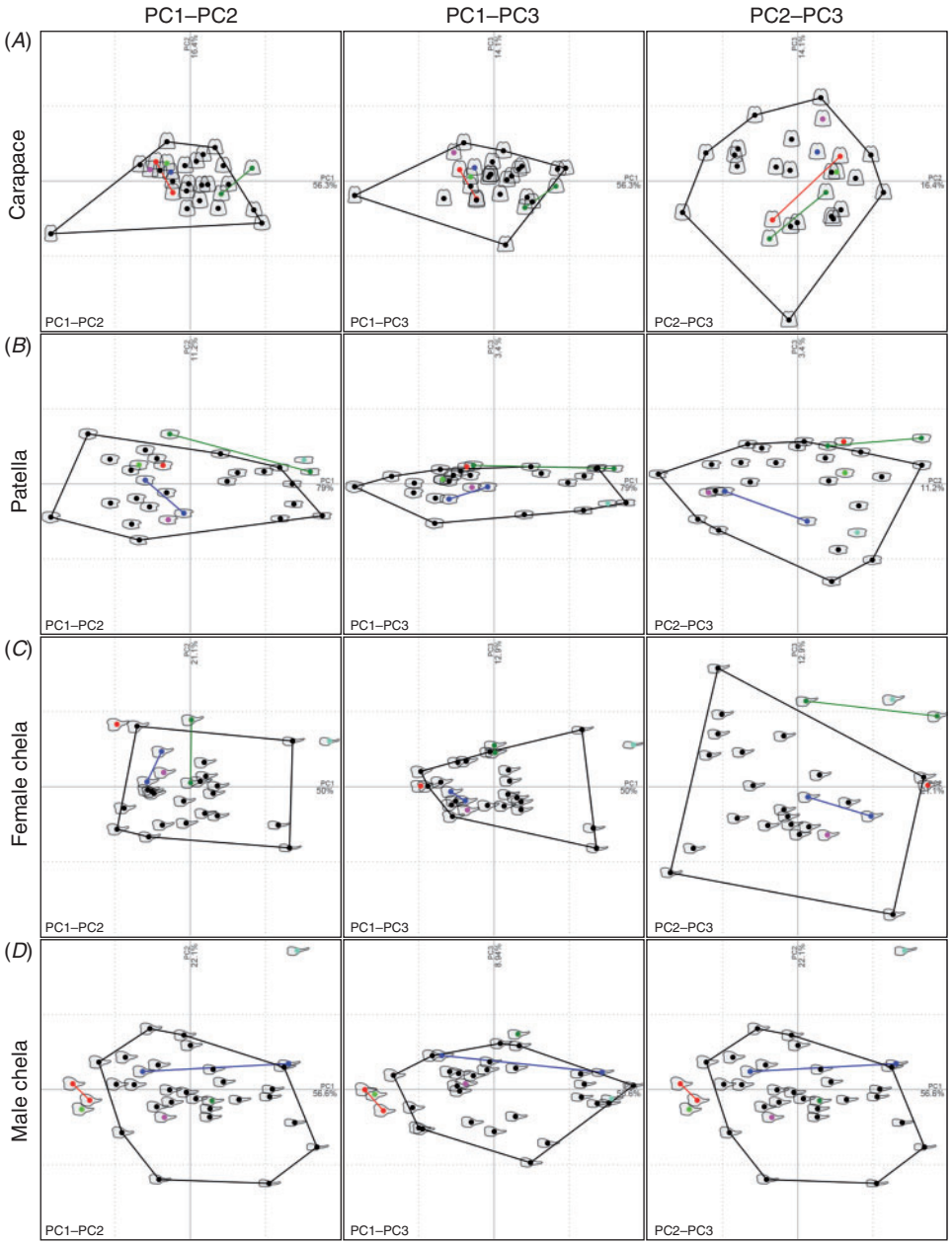

Fig. 3. Visualisation of the morphospaces showing the variation in principal components. Left PC1 versus PC2, centre PC1 versus PC3, right PC2 versus PC3. (*A*) Carapace. (*B*) Retrolateral surface of the pedipalp patella. (*C*) Retrolateral surface of the male pedipalp chela. (*D*) Retrolateral surface of the female pedipalp chela. Colours: *Bioculus* (red), *Didymocentrus* (blue), *Diplocentrus* (black), *Heteronebo* (light green), *Kolotl* (green), *Nebo* (light blue), *Tarsoporosus* (pink). Within *Diplocentrus*: '*zacatecanus*' group (dark cyan), '*keyserlingii*' group (orange), and '*mexicanus*' group (purple).

because of the nested placement of *Kolotl*, *Bioculus* and *Didymocentrus*. The Robinson–Foulds distance calculated was 28 (for a 35-node tree), indicating that these two topologies changed significantly upon the inclusion of only one taxon. Therefore, the proposed characters were not sufficient to resolve the phylogenetic history of Diplocentrinae.

From the 95 discrete morphological characters used by Santibáñez-López *et al.* (2014*a*), 76% evolved randomly according to the ancestral state reconstruction of parsimony steps, whereas 54% evolved randomly under the ancestral state reconstruction using the Mk1 estimates (Fig. 7). Only 35 binary discrete characters were considered as evolving non-randomly either by the parsimony or likelihood ancestral reconstruction. Of those 35 characters, 14 corresponded to leg morphology, eight to pedipalp carination, three to pedipalp chela finger dentition, two to pedipalp trichobothria, three to carapace

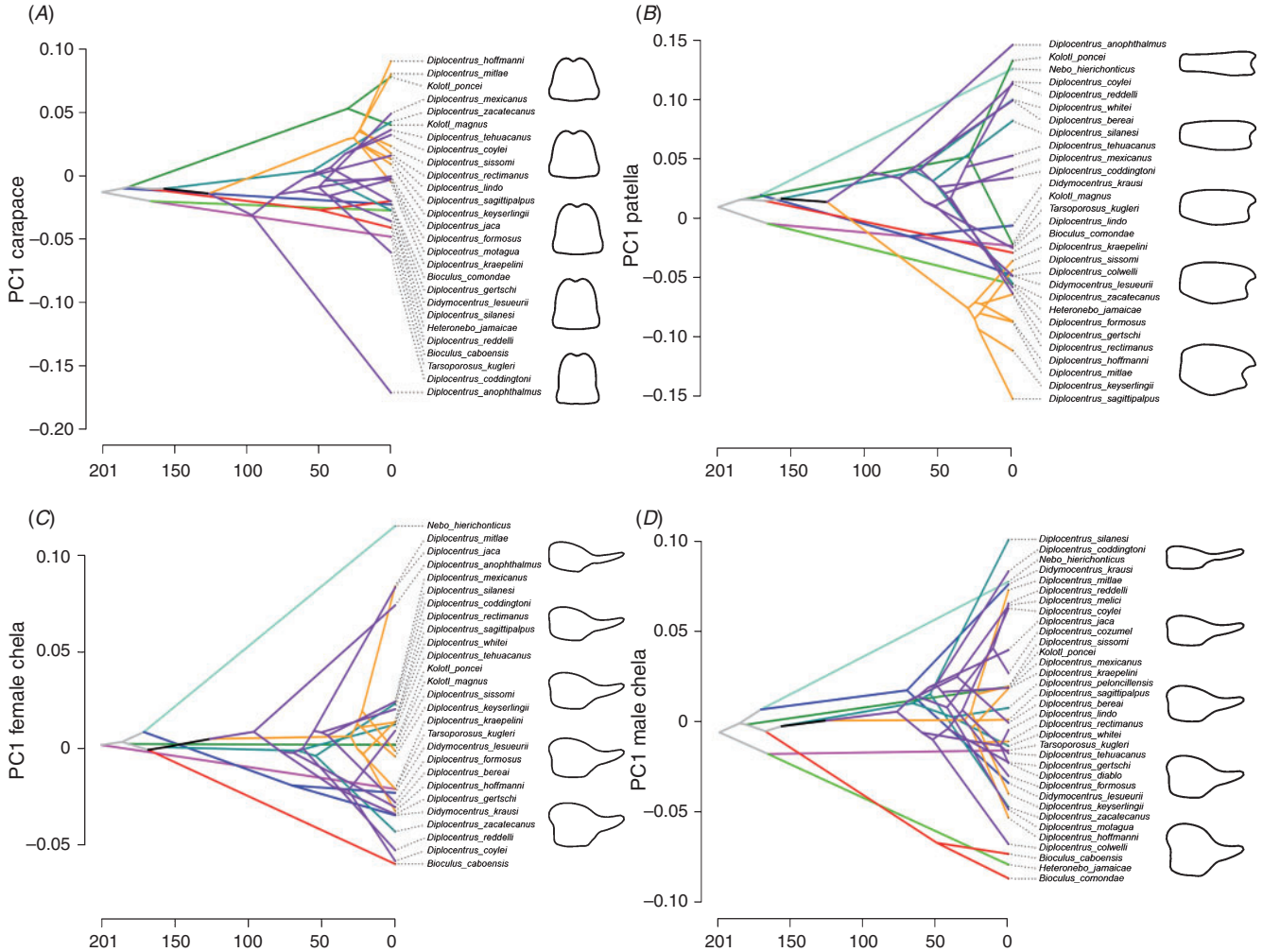

Fig. 4. Visualisation of the PC1 values as a function of phylogenetic relationships recovered from the dated molecular tree from BEAST; *x*-axis indicates the time of divergence, *y*-axis indicates the PC1 values. (*A*) Carapace. (*B*) Retrolateral surface of the pedipalp patella. (*C*) Retrolateral surface of the female pedipalp chela. (*D*) Retrolateral surface of the male pedipalp chela. Colours: *Bioculus* (red), *Didymocentrus* (blue), *Diplocentrus* (black), *Heteronebo* (light green), *Kolotl* (green), *Nebo* (light blue), *Tarsoporosus* (pink). Within *Diplocentrus*: '*zacatecanus*' group (dark cyan), '*keyserlingii*' group (orange), and '*mexicanus*' group (purple).

morphology, two to mesosoma carination/telson surface, and three to pigmentation patterns. Tests of character independence using BayesTraits suggested that characters pertaining to legs, pedipalp chela finger dentition, and pedipalp carination were highly correlated (Tables S3, S4). By contrast, the two pedipalp trichobothria characters (the position of trichobothrium *ib* and *it* on the pedipalp chela manus with a Bayes factor = 0.309), and the mesosoma carina and telson surface (with a Bayes factor = –0.361) were not correlated.

Telotarsal spiniform macrosetae counts have been used to differentiate species in diplocentrid taxonomy, but these counts have never been used in phylogenetic reconstruction or tested in a quantitative framework. Eight telotarsal (t) spiniform macrosetae counts were defined: prolateral (p) and retrolateral (r) counts in each of the four legs (tp1–4, and tr1–4). Telotarsal spiniform counts on tp1, and tr1–2 showed significant phylogenetic signal according to the Abouheif C_{mean} index (Fig. 8), whereas tp2–4, and tr3–4 were more conserved. On the other hand, λ and *K* indices showed that, whereas tp1–2, and tr1–4, had significant values consistent with the phylogenetic structure, only tp3 and tp4 reflected strong conservation of these counts in most diplocentrids (Table 1). However, all the counts with strong phylogenetic signal were recovered as strongly correlated by BayesTraits (Tables S5, S6).

Unlike telotarsal spiniform macrosetae, basitarsal spiniform macrosetae were not considered in diplocentrid systematics until recently. Hypotheses relating to the homology of these setae have been presented before (e.g. Santibáñez-López *et al.* 2014*a*), showing great utility for differentiating lineages at the genus and species levels. However, one of the main difficulties in establishing homology hypotheses across setae is the absolute position of these structures. For this reason, they are identified by their position relative to a landmark (e.g. Agolin and D'Haese 2009). These characters were also included in the BayesTraits analysis of discrete traits, though we analysed them also as continuous characters. The basitarsal (b) spiniform

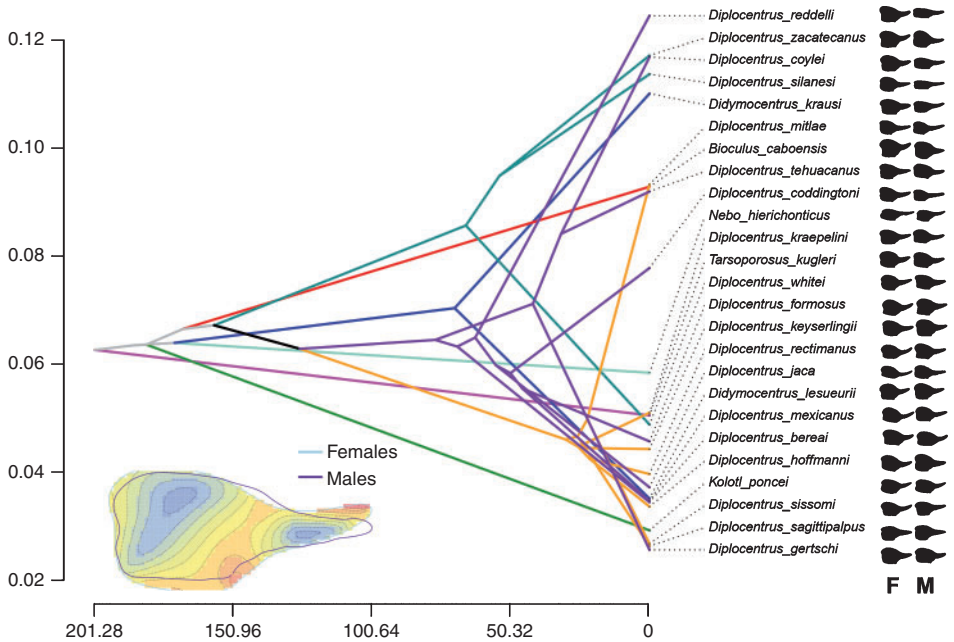

Fig. 5. Visualisation of the Euclidean distances as a measure of the variation of morphology in the sexual dimorphism of male and female pedipalp chelae onto the dated molecular tree from BEAST; *x*-axis indicates the time of divergence, *y*-axis indicates the Euclidean distance. To the right, composite images of the chelae of females and males. Basal superimposed chelae showing the heat map on most important changes between both chelae: delimited chela represents the one from males, whereas the coloured represents the one from the female. Colours: *Bioculus* (red), *Didymocentrus* (blue), *Diplocentrus* (black), *Heteronebo* (light green), *Kolotl* (green), *Nebo* (light blue), *Tarsoporosus* (pink). Within *Diplocentrus*: '*zacatecanus*' group (dark cyan), '*keyserlingii*' group (orange), and '*mexicanus*' group (purple).

formulae of legs I, II and III were chosen (leg IV is almost identical to leg III, as explained in Santibáñez-López *et al*. 2013*a*, 2013*b*; Santibáñez-López and Francke 2013) as follows: distal (d), subdistal (sd), medial (m), proximal (pr), retrolateral (r). Five counts (b1d, b1sd, b1m, b1rm and b1rpr) for the basitarsus of leg I, six counts (b2d, b2sd, 2bm, b2rd, b2rm and b2rpr) for basitarsus of leg II and three counts for leg III (b3d, b3sd and b3m) were considered (Table S2). Counts on b1rpr, b2rd, b2rm, b2rpr, b3sd and b3m showed strong phylogenetic signal according to the three indices (Fig. 8; Table 2); whereas b3d was conserved across the entire family. However, some of these characters were correlated, according to the BayesTraits analysis (e.g. b1rpr and b2rpr: see Table S6).

The variation of these counts between diplocentrids in the PCA is shown in Fig. 9. PC1 for the telotarsal counts explained 85.7% of the variation, and it accounted for the spiniform macrosetae counts on tp4 and tr4 (Fig. 9*A*). *T. kugleri* and *N. hierichonticus* were at extreme opposites in character state value, with the lowest and highest counts (respectively). PC2 explained 5.3% and PC3 3.7% of the variation, accounting for the counts on tp2–3, and tr2–3 (PC2), and counts on tp1 and tr1 (PC3). Both species of *Didymocentrus* were separated from the rest of the diplocentrids by these two PCs. The phenogram of PC1 indicated the higher telotarsal counts in *Nebo* originated early in the evolution of diplocentrid scorpions (Fig. S3*A*). On the other hand, the variation of the basitarsal counts was not as high as for the telotarsal counts. PC1 explained 24.1% of the variation and it accounted for the counts on b1m, b1rpr, b2m, b2rm and b2rpr (Fig. S3*B*). *N. hierichonticus* was the only species separated from the rest of the diplocentrids in this morphospace, being the only species with one seta on b1rpr and b2rpr. Finally, PC2 and PC3 explained 17.4% and 13.2% (respectively) of the variation in the rest of the counts, separating *N. hierichonticus* from the rest of the diplocentrids.

Discussion

The status of subfamilies Nebinae and Diplocentrinae

This study represents the first assessment of the monophyly of the Diplocentridae and its constituent lineages, using molecular sequence data exclusively. Our results showed that Diplocentridae is monophyletic; however, the sister relationship between Scorpionidae and Diplocentridae was not favoured in our analysis, as suggested earlier (i.e. Sharma *et al*. 2015). Within Diplocentridae, the monophyly of subfamily Diplocentrinae was not recovered in any of our analyses, because *N. hierichonticus* was never recovered as the sister group taxon to the rest of the diplocentrid genera, but instead was always embedded within the Diplocentrinae. Furthermore, the inclusion of *N. hierichonticus* in the morphological matrix and the reanalysis of this matrix resulted in the collapse of Diplocentrinae monophyly, suggesting that these characters are highly homoplastic across Diplocentridae.

The phylogenetic position of *N. hierichonticus* within Diplocentrinae was also favoured by the morphometric

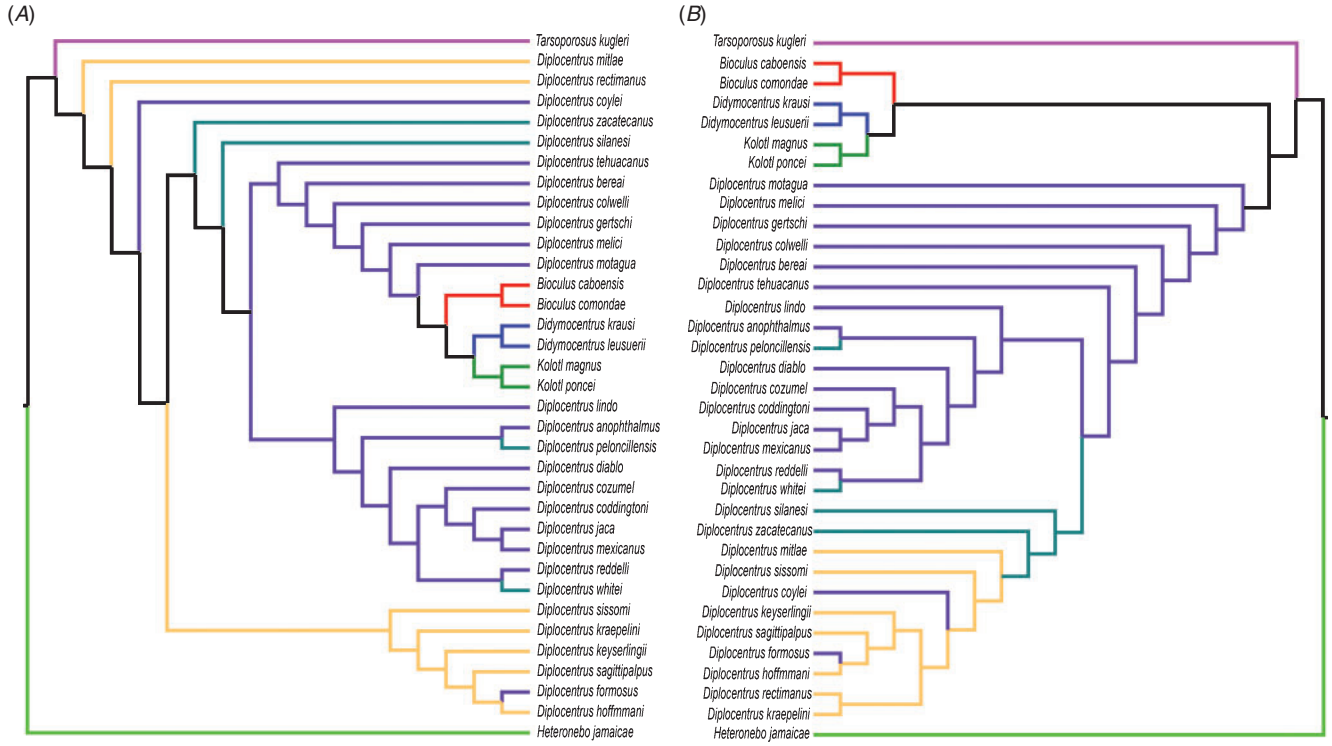

Fig. 6. The most parsimonious trees recovered from the analysis of the 95 morphological characters with implied weights and constant *k* value of 100. (*A*) Tree topology recovered by the analysis with the inclusion of *N. hierichonticus*, but trimmed for comparative purposes. (*B*) Tree topology recovered by an earlier analysis (Santibañez-López *et al*. 2014*a*). The Robison–Foulds distance between them was 28. Colours: *Bioculus* (red), *Didymocentrus* (blue), *Diplocentrus* (black), *Heteronebo* (light green), *Kolotl* (green), *Nebo* (light blue), *Tarsoporosus* (pink). Within *Diplocentrus*: '*zacatecanus*' group (dark cyan), '*keyserlingii*' group (orange), and '*mexicanus*' group (purple).

analyses. The pedipalp patella shape of *N. hierichonticus* and the rest of the diplocentrids overlapped in the three principal components, whereas only the shape of the male pedipalp chela of *N. hierichonticus* on PC1 separated this species from the rest. Also, the morphometric analyses of the tarsal spiniform macrosetae counts on the legs showed great overlap between *N. hierichonticus* and the rest of the diplocentrine species. The monophyly of the genus *Nebo* has not been tested before. The nine species included in this genus are problematic because they were diagnosed on the basis of morphometric ratios based on few specimens (e.g. Francke 1980; Sissom 1994; Hendrixson 2006), and characters previously used in diplocentrid systematics have proved not to be useful in *Nebo* (Francke 1980).

The nested phylogenetic position of *N. hierichonticus* in our analyses suggests that subfamily Nebinae is a synonym of Diplocentrinae, and that various characters that distinguish Nebinae from the remaining diplocentrids actually constitute synapomorphies of the morphologically atypical genus *Nebo* (e.g. the position of the trichobotrium *it* distal to *ib* on pedipalp chela manus; higher telotarsal spiniform macrosetae counts). This inference is supported by the large degree of overlap in morphospace between *Nebo* and the other genera, for several character systems, and the inefficiency of the mainstay characters in Diplocentridae (e.g. pedipalp morphosculpture) to resolve its phylogenetic position. In order to render Diplocentrinae monophyletic, we treat Nebinae as a junior synonym of Diplocentrinae (**new synonymy**).

It was beyond the scope of this study to analyse the phylogenetic relationships of all the diplocentrid genera, due to the absence of representatives of three Caribbean genera (*Cazierius*, *Cryptoiclus* and *Oiclus*). However, the inclusion of *Nebo* in these analyses showed that the relationship (*Bioculus* + *Diplocentrus*) was stable, as previously recognised (Santibáñez-López *et al*. 2014*a*). Within *Diplocentrus*, the relationships between the three groups were consistent with the previous study except for the position of *D. zacatecanus*, which is likely due to the removal of two sequences (*12S* and *COI*) for this species. However, the phylogenetic position of *D. zacatecanus*, as sister taxon to *D. whitei* and *D. peloncillensis*, is congruent with the geographical distribution of these species.

The utility of morphometrics and general morphology in diplocentrid taxonomy

This study examined for the first time the evolution of shape as a continuous trait in a family of scorpions, in order to test the systematic utility of taxonomic ranks (subfamilies), and examine the evolution of sexual dimorphism with reference to a multilocus molecular phylogeny. Traditional morphometrics (e.g. ratios) have been used several times to diagnose and differentiate scorpion genera and species (e.g. Francke 1978), but scorpion external shape has not been examined in a parametric manner, and thus the phylogenetic utility of this

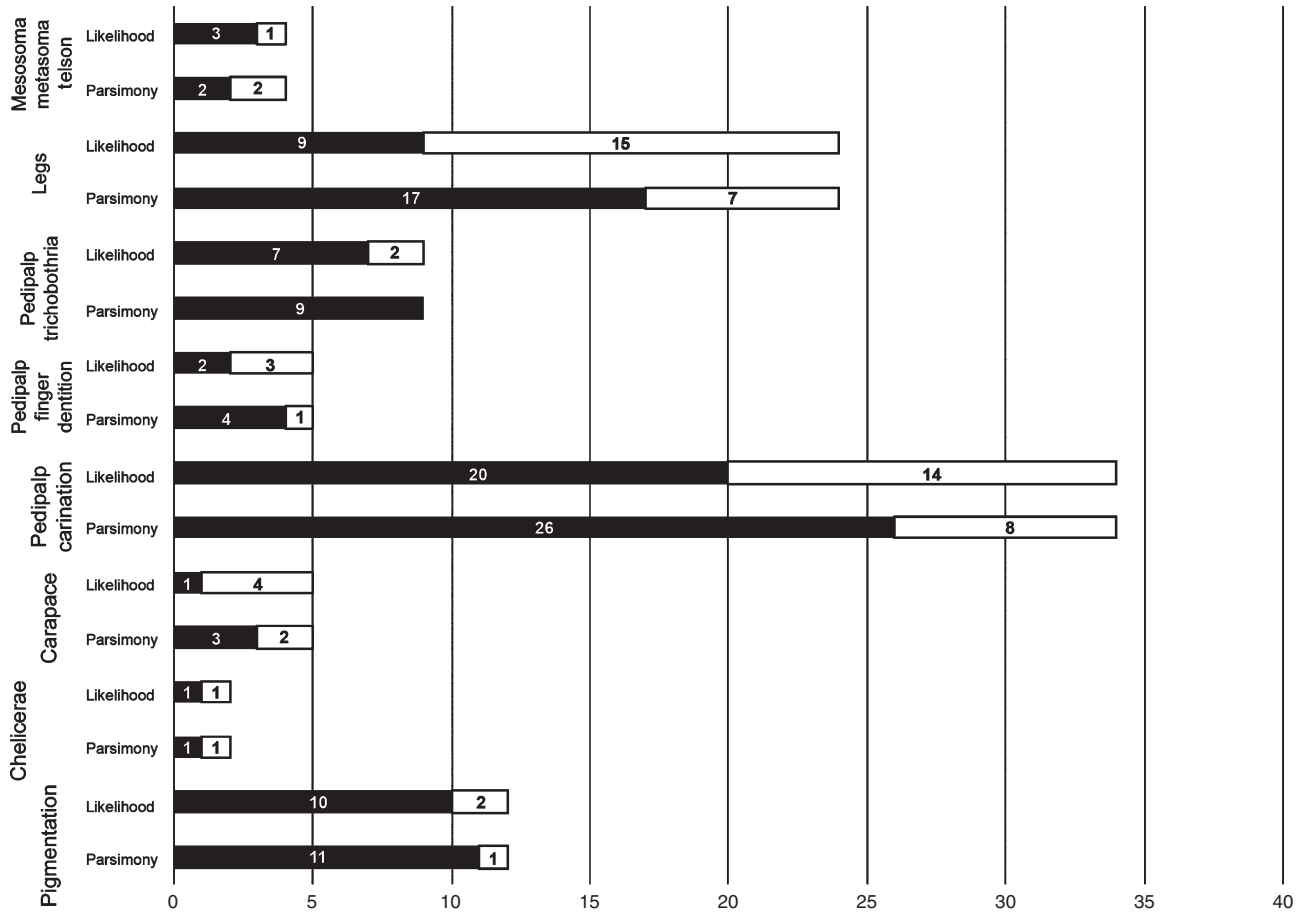

Fig. 7. Distribution of the uninformative (black) versus the informative (white) characters from the morphological matrix from Santibáñez-López *et al.* (2014*a*). Characters are partitioned by character system; maximum-likelihood and parsimony permutation test outcomes are shown.

character class is unknown. Our multivariate analysis of the shape data, plus the analyses of the phylogenetic signal in the discrete characters used in the previous analysis (i.e. Santibáñez-López *et al*. 2014*a*), revealed their convergent evolution at different hierarchical levels (e.g. subfamily, genus and species groups) within the Diplocentridae. The morphology of the carapace did not show significant differences across genera, except for *D. anophthalmus*, which is likely correlated with the global troglomorphic morphology of this species, as seen in other distantly related troglobitic scorpions (e.g. *Alacran tartarus*, *Typhlochactas sissomi*). The shape of the anterior median notch (i.e. depth) showed overlapping groups across the three species groups within *Diplocentrus*, supporting its validity for diagnosing species, as previously recognised (e.g. Santibáñez-López *et al*. 2013*a*, 2013*b*; Santibáñez-López 2014), but not as a diagnostic character for genera.

The results of the analysis of the retrolateral surface of the pedipalp patella showed that the length–width ratio accounted for the greatest proportion of variation (79%), as accounted for by PC1. Even when this ratio was prone to broad overlap across genera, its utility in *Diplocentrus* taxonomy is corroborated. This ratio split the '*keyserlingii*' group from the '*mexicanus*' and '*zacatecanus*' groups, with convergence in some species of these two groups (e.g. *D. formosus*, *D. coylei*, which were originally placed in the '*keyserlingii*' group). Therefore, this ratio can also be used to diagnose members of the '*keyserlingii*' group along with the others previously reported (Santibáñez-López *et al*. 2013*a*).

Variation in the morphology of the pedipalp chela of males and females revealed high homoplasy and was prone to broad overlap across genera and species groups in the Diplocentridae. Therefore, significant differences between genera or species groups with taxonomic utility (i.e. clustering in accordance with phylogenetic distance) were not found. Our analysis showed that sexual dimorphism in the shape of the pedipalp chela has evolved multiple times in the Diplocentridae. While *B. caboensis* and *Di. krausi* were the only representatives outside *Diplocentrus* with strong sexual dimorphism (Euclidean distance >0.60); *Di. lesueurii*, *K. poncei*, *N. hierichonticus* and *T. kugleri* did not show strong sexual dimorphism in the shape of the chela. Within *Diplocentrus*, sexual dimorphism in the shape of the chela has evolved several times, in each of the three groups. For example, while *D. mitlae* was the only member of the '*keyserlingii*' group presenting significant sexual dimorphism in the overall shape of the pedipalp chela, *D. whitei* was the only species of the '*zacatecanus*' without significant sexual dimorphism. In contrast, sexual dimorphism has evolved several times within the '*mexicanus*' group, suggesting a

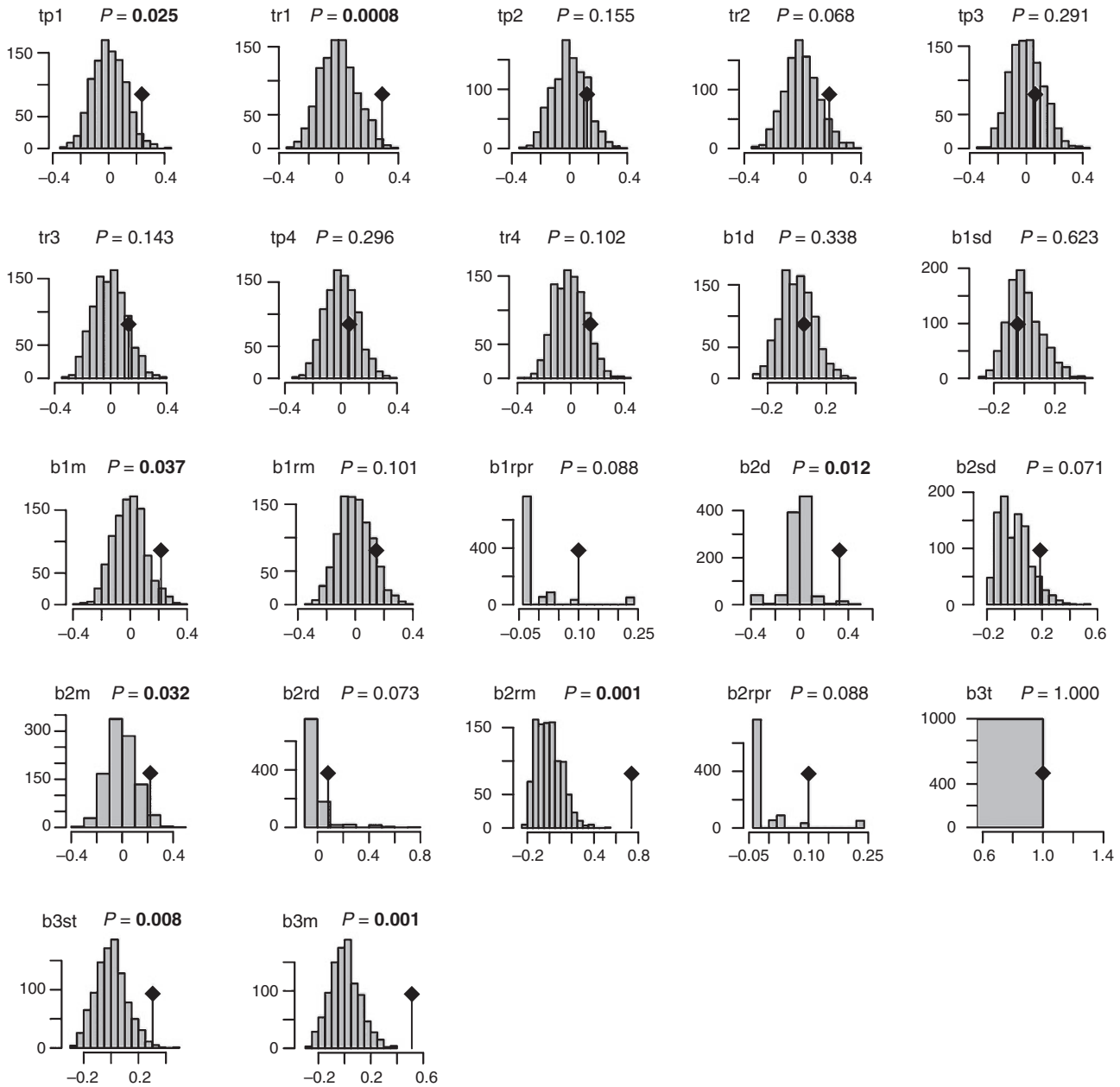

Fig. 8. Histogram of the frequency distribution of the Aboheif C_{mean} calculated from the tarsal spiniform macrosetae counts for the diplocentrid scorpion species in the phylogeny. Vertical line indicates the observed C_{mean} relative to the null hypothesis sampling distribution of randomised C_{mean}. Parameters exhibiting phylogenetic signal are indicated by their *P* value in bold.

utility as a diagnostic character in species descriptions, but not as a generic diagnostic character.

Tarsal macrosetae have high phylogenetic signal and constitute multiple character systems

Telotarsal spiniform macrosetal counts in walking legs are central components in diplocentrid systematics. However, neither their phylogenetic signal nor their variation has been tested using parametric approaches. Our PC analyses showed that while the variation of the telotarsal spiniform macrosetal counts are a reliable generic diagnostic character system, the variation of the basitarsal setal counts are not, because of greater overlap. Our analyses also showed that telotarsal counts retain phylogenetic signal, higher on the telotarsal setal counts of the retrolateral face of legs I and II than on the legs III and IV. Telotarsal setal counts of the prolateral face of legs I and II also retain phylogenetic signal, but on legs III and IV do not.

Despite the clear phylogenetic signal of six (out of the eight) telotarsal setal counts traditionally used in diplocentrid systematics, all of them showed strong correlation. This correlation was stronger between the counts on the retrolateral

face of legs III and IV, and between the counts on the prolateral face of leg II and the retrolateral face of legs III and IV. Finally, basitarsal spiniform setal counts on leg III, either if they are treated as discrete characters or as counts, retain phylogenetic

Table 1. Correspondence of telotarsal spiniform macrosetae counts and their phylogenetic signal
Boldface text indicates significant values

	Pagel's λ				Blomerg *et al.*'s *K*	
	λ	LogL	$LogL_0$	*p*	*K*	*p*
tp1	**0.831**	–38.588	–44.337	**0.001**	0.606	0.002
tr1	**0.932**	–45.466	–54.280	**0.000**	0.725	0.001
tp2	**0.802**	–41.917	–44.518	**0.023**	0.433	0.025
tr2	**0.978**	–47.706	–53.520	**0.001**	0.627	0.001
tp3	0.560	–45.099	–45.434	0.412	0.295	0.317
tr3	**0.879**	–48.913	–53.115	**0.004**	0.497	0.008
P4	0.786	–42.953	–44.011	0.146	0.424	0.029
R4	**0.888**	–51.302	–54.785	**0.008**	0.496	0.009

Table 2. Correspondence of basitarsal spiniform macrosetae counts and their phylogenetic signal
Boldface text indicates significant values. –, not applicable

	Pagel's λ				Blomerg *et al.*'s *K*	
	λ	LogL	$LogL_0$	*P*	*K*	*P*
b1d	0.000	–45.736	–45.736	1.000	0.248	0.514
b1sd	0.000	–35.588	–35.588	1.000	0.314	0.260
b1m	0.452	–38.747	–40.401	0.069	0.293	0.304
b1rm	0.088	–24.696	–24.683	1.000	0.330	0.188
b1rpr	**1.029**	35.777	13.929	**0.000**	1.421	0.084
b2d	0.000	–6.186	–6.186	1.000	0.307	0.397
b2sd	0.000	–17.713	–17.713	1.000	0.400	0.091
b2m	0.463	–42.910	–45.736	0.017	0.300	0.253
b2rd	**1.029**	8.244	1.974	**0.000**	0.641	0.083
b2rm	**1.029**	18.299	–19.485	**0.000**	4.970	0.001
b2rpr	**1.029**	35.777	13.929	**0.000**	1.421	0.086
b3d	0.753	1258.463	–	–	6.613	1.000
b3sd	**0.755**	–20.566	–24.008	**0.009**	0.443	0.017
b3m	**1.029**	–8.892	–25.621	**0.000**	1.029	0.001

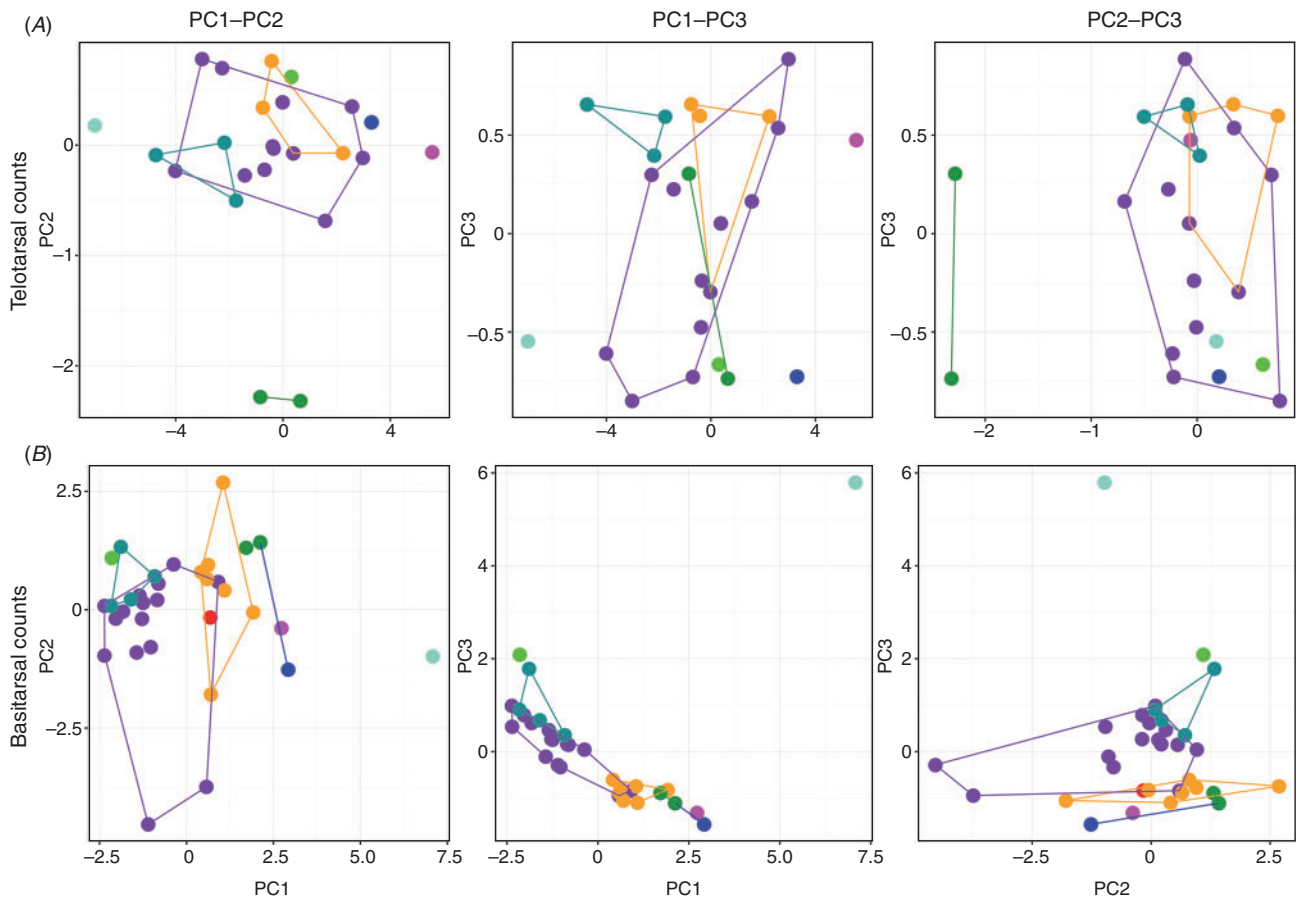

Fig. 9. Visualisation of the counts showing the variation in principal components. Left PC1 versus PC2, centre PC1 versus PC3, right PC2 versus PC3. (*A*) Telotarsal spiniform macrosetae counts. (*B*) Basitarsal spiniform macrosetae counts. Colours: *Bioculus* (red), *Didymocentrus* (blue), *Diplocentrus* (black), *Heteronebo* (light green), *Kolotl* (green), *Nebo* (light blue), *Tarsoporosus* (pink). Within *Diplocentrus*: '*zacatecanus*' group (dark cyan), '*keyserlingii*' group (orange), and '*mexicanus*' group (purple).

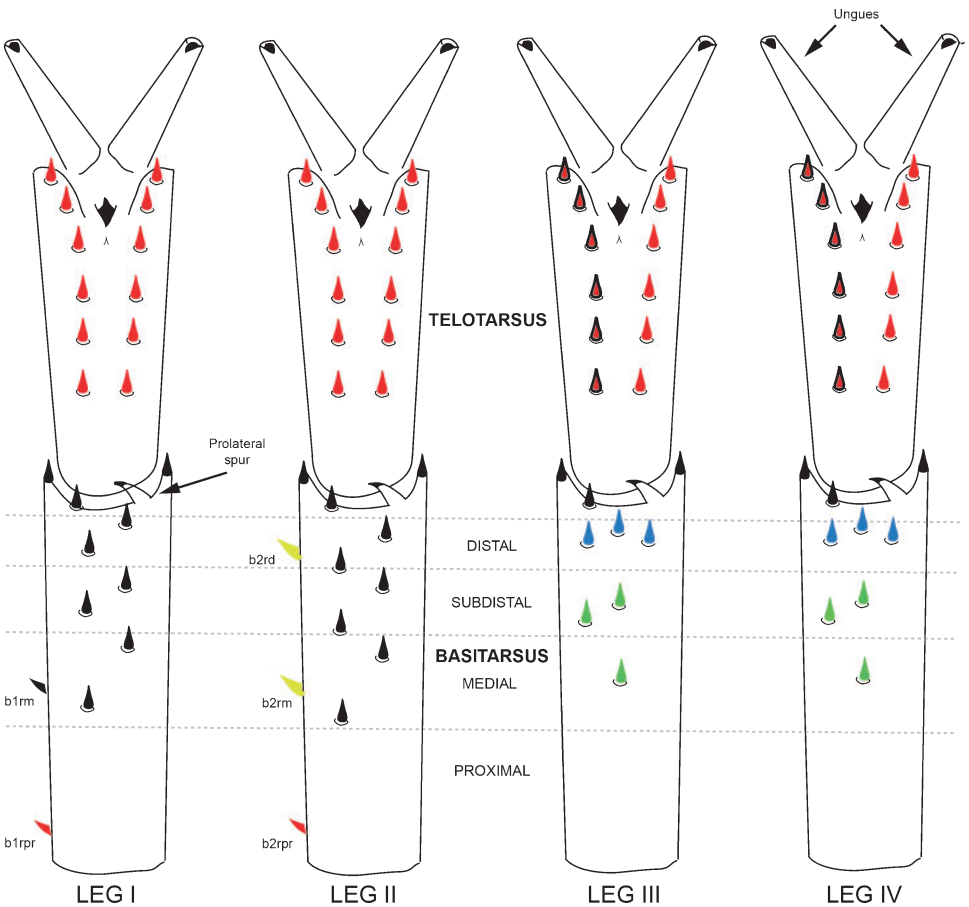

Fig. 10. Composite scheme for the telotarsal and basitarsal counts systems based on specimens of the diplocentrid species studied here. Leg IV is identical to leg III. Colours represent systems as follows: red includes the telotarsal counts (also b1rpr and b2rpr) highly correlated with each other; red with black border retains no phylogenetic signal; yellow includes setae b2rd and b2rm, both retain phylogenetic signal; green includes b3sd and b3m, both retain phylogenetic signal; blue includes b3d (which were constant across the entire family and are useful for family diagnoses); and black includes those setae from legs I and II that retain no phylogenetic signal, but may serve as species diagnostic characters.

signal, but also are correlated. This would suggest that counting setae, instead of identifying setae by name, would also be reliable characters.

By examining both phylogenetic signal and trait correlation within these counts, we are able to circumscribe five independent character systems within the telotarsal and basitarsal spiniform setal counts, as well as quantify their informativeness (Fig. 10), as follows: (1) the telotarsal counts on all legs (for all diplocentrids) and the presence of b1rpr and b2rpr (unique to *N. hierichonticus*); (2) the presence of b2rd and b2rm; (3) the counts on the subdistal and medial basitarsus of legs III–IV; (4) the three spiniform macrosetae on the distal basitarsus of leg III–IV (constant to all diplocentrids: this study; CESL, unpubl. data); and (5) the counts on the basitarsus of legs I–II. Future studies should test whether this degree of character independence between the telotarsus and basitarsus holds for other scorpion family-level groups, as well as deploy such methods to other character-state-rich morphological data structures, such as trichobothrial patterns.

Conclusions

Here we inferred a multilocus phylogeny for Diplocentridae, which allowed us to test the monophyly of the family and the integrity of the subfamilial nomenclature. Using this phylogeny as a framework for inference of morphological character evolution, we quantified the systematic utility and character dependence of discrete and continuous character systems, and examined the evolution of shape for the first time using parametric methods. We demonstrated the monophyly of the family, and our dataset justified the synonymy of the two subfamilies. Visualisation of sexual dimorphism in the pedipalp chela manus shows that highly divergent sexual morphs have evolved repeatedly within the Diplocentridae. We also showed that morphology exhibits great homoplasy within the Diplocentridae, and we demonstrated that tarsal spiniform macrosetae counts should remain a mainstay of diplocentrid systematics, albeit with consideration of patterns of character dependence.

Acknowledgements

We are greatly indebted to Diego Barrales, Kevin Sagastume and Jan Rein, who kindly provided us with some of the images used in this contribution. CESL was supported by a postdoctoral CONACYT grant (reg. 207146/454834). RK was supported by the Dimensions of Biodiversity program (award DEB-1046355). PPS was supported by an NSF CAREER grant (IOS-1552610).

References

Abouheif, E. (1999). A method for testing the assumption of phylogenetic independence in comparative data. *Evolutionary Ecology Research* **1**, 895–909.

Agolin, M., and D'Haese, C. A. (2009). An application of dynamic homology to morphological characters: direct optimization of setae sequences and phylogeny of the family Odontellidae (Poduromorpha, Collembola). *Cladistics* **25**, 353–385. doi:10.1111/j.1096-0031.2009.00272.x

Blomberg, S. P., Garland, T., and Ives, A. R. (2003). Testing for phylogenetic signal in comparative data: behavioral traits are more labile. *Evolution* **57**, 717–745. doi:10.1111/j.0014-3820.2003.tb00285.x

Bonhomme, V., Picq, S., Gaucherel, C., and Claude, J. (2014). Momocs: outline analysis using R. *Journal of Statistical Software* **56**, 1–24. doi:10.18637/jss.v056.i13

Castresana, J. (2000). Selection of conserved blocks from multiple alignments for their use in phylogenetic analysis. *Molecular Biology and Evolution* **17**, 540–552. doi:10.1093/oxfordjournals.molbev.a026334

Chessel, D., Dufour, A. B., and Thioulouse, J. (2004). The ade4 package-I-one-table methods. *R News* **4**, 5–10.

Coddington, J. A., Giribet, G., Harvey, M. S., Prendini, L., and Walter, D. E. (2004). Arachnida. In 'Assembling the Tree of Life'. (Eds J. Cracraft and P. C. J. Donoghue.) pp. 296–318. (Oxford University Press: New York.)

Darriba, D., Taboada, G. L., Doallo, R., and Posada, D. (2012). jModelTest 2: more models, new heuristics and parallel computing. *Nature Methods* **9**, 772. doi:10.1038/nmeth.2109

Drummond, A. J., Ho, S., Phillips, M. J., and Rambaut, A. (2006). Relaxed phylogenetics and dating with confidence. *PLoS Biology* **4**(5), e88. doi:10.1371/journal.pbio.0040088

Drummond, A. J., Suchard, M. A., Xie, D., and Rambaut, A. (2012). Bayesian phylogenetics with BEAUti and the BEAST 1.7. *Molecular Biology and Evolution* **29**, 1969–1973. doi:10.1093/molbev/mss075

Edgar, R. C. (2004). MUSCLE: multiple sequence alignment with high accuracy and high throughput. *Nucleic Acids Research* **32**, 1792–1797. doi:10.1093/nar/gkh340

Fet, V., Gantenbein, B., Gromov, A., Lowe, G., and Lourenço, W. R. (2003). The first molecular phylogeny of Buthidae (Scorpiones). *Euscorpius* **4**, 1–10.

Francke, O. F. (1977*a*). Taxonomic observations on *Heteronebo* Pocock (Scorpionida, Diplocentridae). *The Journal of Arachnology* **4**, 95–113.

Francke, O. F. (1977*b*). Scorpions of the genus *Diplocentrus* from Oaxaca, Mexico (Scorpionida, Diplocentridae). *The Journal of Arachnology* **4**, 145–200.

Francke, O. F. (1978). Systematic revision of diplocentrid scorpions (Diplocentridae) from circum-Caribbean lands. *Special Publications The Museum Texas Tech University* **14**, 1–92.

Francke, O. F. (1980). Revision of the genus *Nebo* Simon (Scorpiones: Diplocentridae). *The Journal of Arachnology* **8**, 35–52.

Francke, O. F., and Prendini, L. (2008). Phylogeny and classification of the giant hairy scorpions, *Hadrurus* Thorell (Iuridae Thorell): a reappraisal. *Systematics and Biodiversity* **6**, 205–223. doi:10.1017/S1477200008002697

Francke, O. F., Teruel, R., and Santibáñez-López, C. E. (2014). A new genus and a new species of scorpion (Scorpiones: Buthidae) from southeastern Mexico. *The Journal of Arachnology* **42**, 220–232. doi:10.1636/Ha13-33.1

Goloboff, P. A., Farris, J. S., and Nixon, K. C. (2008). TNT, a free program for phylogenetic analysis. *Cladistics* **24**, 774–786. doi:10.1111/j.1096-0031.2008.00217.x

González-Santillán, E., and Prendini, L. (2015). Phylogeny of the North American vaejovid scorpion subfamily Syntropinae Kraepelin, 1905, based on morphology, mitochondrial and nuclear DNA. *Cladistics* **31**, 341–405. doi:10.1111/cla.12091

Guindon, S., and Gascuel, O. (2003). A simple, fast, and accurate algorithm to estimate large phylogenies by maximum likelihood. *Systematic Biology* **52**, 696–704. doi:10.1080/10635150390235520

Hendrixson, B. E. (2006). Buthid scorpions of Saudi Arabia, with notes on other families (Scorpiones: Buthidae, Liochelidae, Scorpionidae). *Fauna of Saudi Arabia* **21**, 33–120.

Keck, F., Rimet, F., Bouchez, A., and Franc, A. (2016). phylosignal: an R package to measure, test, and explore the phylogenetic signal. *Ecology and Evolution* **6**, 2774–2780. doi:10.1002/ece3.2051

Maddison, W. P., and Maddison, D. R. (2016). Mesquite: a modular system for evolutionary analysis. Version 3.10. Available at http://mesquiteproject.org.

Mattoni, C., Ochoa, J., Ojanguren-Affilastro, A., and Prendini, L. (2010). Towards an all-species phylogeny of the scorpion family Bothriuridae. *Cladistics* **26**, 216–217.

Monod, L., and Prendini, L. (2015). Evidence for Eurogondwana: the roles of dispersal, extinction and vicariance in the evolution and biogeography of Indo-Pacific Hormuridae (Scorpiones: Scorpionoidea). *Cladistics* **31**, 71–111. doi:10.1111/cla.12067

Münkemüller, T., Lavergne, S., Bzeznik, B., Dray, S., Jombart, T., Schiffers, K., and Thuiller, W. (2012). How to measure and test phylogenetic signal. *Methods in Ecology and Evolution* **3**, 743–756. doi:10.1111/j.2041-210X.2012.00196.x

Ojanguren-Affilastro, A. A., Mattoni, C. I., Ochoa, J. A., Ramírez, M. J., Ceccarelli, F. S., and Prendini, L. (2016). Phylogeny, species delimitation and convergence in the South American bothriurid scorpion genus *Brachistosternus* Pocock 1893: integrating morphology, nuclear and mitochondrial DNA. *Molecular Phylogenetics and Evolution* **94**, 159–170. doi:10.1016/j.ympev.2015.08.007

Pagel, M. (1999). Inferring the historical patterns of biological evolution. *Nature* **401**, 877–884. doi:10.1038/44766

Pagel, M., and Meade, A. (2006). Bayesian analysis of correlated evolution of discrete characters by reversible-jump Markov Chain Monte Carlo. *American Naturalist* **167**, 808–825.

Pavoine, S., Ollier, S., Pontier, D., and Chessel, D. (2008). Testing for phylogenetic signal in phenotypic traits: new matrices of phylogenetic proximities. *Theoretical Population Biology* **73**, 79–91. doi:10.1016/j.tpb.2007.10.001

Posada, D., and Buckley, T. R. (2004). Model selection and model averaging in phylogenetics: advantages of Akaike information criterion and Bayesian approaches over likelihood ratio tests. *Systematic Biology* **53**, 793–808. doi:10.1080/10635150490522304

Prendini, L. (2000). Phylogeny and classification of the superfamily Scorpionoidea Latreille 1802 (Chelicerata, Scorpiones): an exemplar approach. *Cladistics* **16**, 1–78. doi:10.1111/j.1096-0031.2000.tb00348.x

Prendini, L. (2003). A new genus and species of bothriurid scorpion from the Brandberg Massif, Namibia, with a reanalysis of bothriurid phylogeny and a discussion of the phylogenetic position of *Lisposoma* Lawrence. *Systematic Entomology* **28**, 149–172. doi:10.1046/j.1365-3113.2003.00207.x

Prendini, L., and Esposito, L. A. (2010). A reanalysis of *Parabuthus* (Scorpiones: Buthidae) phylogeny with descriptions of two new

Parabuthus species endemic to the Central Namib gravel plains, Namibia. *Zoological Journal of the Linnean Society* **159**, 673–710.

Prendini, L., and Wheeler, W. C. (2004). Assembling the scorpion tree of life: phylogeny of extant scorpions based on molecules, morphology and exemplars. *Cladistics* **20**, 602–603.

Prendini, L., Crowe, T. M., and Wheeler, W. C. (2003). Systematics and biogeography of the family Scorpionidae (Chelicerata: Scorpiones), with a discussion on phylogenetic methods. *Invertebrate Systematics* **17**, 185–259. doi:10.1071/IS02016

Prendini, L., Francke, O. F., and Vignoli, V. (2010). Troglomorphism, trichobothriotaxy and typhlochactid phylogeny (Scorpiones, Chactoidea): more evidence that troglobitism is not an evolutionary dead-end. *Cladistics* **26**, 117–142. doi:10.1111/j.1096-0031.2009.00277.x

Rambaut, A., Suchard, M. A., Xie, D., and Drummond, A. J. (2014). Tracer v1.6. Available at http://beast.bio.ed.ac.uk/Tracer.

Revell, L. J. (2012). phytools: an R package for phylogenetic comparative biology (and other things). *Methods in Ecology and Evolution* **3**, 217–223. doi:10.1111/j.2041-210X.2011.00169.x

Robinson, D. F., and Foulds, L. R. (1981). Comparison of phylogenetic trees. *Mathematical Biosciences* **53**, 131–147. doi:10.1016/0025-5564(81)90043-2

Ronquist, F., Teslenko, M., van der Mark, P., Ayres, D. L., Darling, A., Höhna, S., Larget, B., Liu, L., Suchard, M. A., and Huelsenbeck, J. P. (2012). MrBayes 3.2: efficient Bayesian phylogenetic inference and model choice across a large model space. *Systematic Biology* **61**, 539–542. doi:10.1093/sysbio/sys029

Santibáñez-López, C. E. (2014). A new species of the genus *Diplocentrus* Peters, 1861 (Scorpiones, Diplocentridae) from Oaxaca, Mexico. *ZooKeys* **412**, 103–116. doi:10.3897/zookeys.412.7619

Santibáñez-López, C. E., and Francke, O. F. (2013). Redescription of *Diplocentrus zacatecanus* (Scorpiones: Diplocentridae) and limitations of the hemispermatophore as a diagnostic trait for genus *Diplocentrus*. *The Journal of Arachnology* **41**, 1–10. doi:10.1636/Ha12-65.1

Santibáñez-López, C. E., Francke, O. F., and Prendini, L. (2013*a*). Systematics of the *keyserlingii* group of *Diplocentrus* Peters, 1861 (Scorpiones: Diplocentridae), with descriptions of three new species from Oaxaca, Mexico. *American Museum Novitates* **3777**, 1–48. doi:10.1206/3777.2

Santibáñez-López, C. E., Francke, O. F. B., and Ortega-Gutierrez, A. (2013*b*). Variation in the spiniform macrosetae pattern on the basitarsi of *Diplocentrus tehuacanus* (Scorpiones: Diplocentridae): new characters to diagnose species within the genus. *The Journal of Arachnology* **41**, 319–326. doi:10.1636/Ha13-12.1

Santibáñez-López, C. E., Francke, O. F., and Prendini, L. (2014*a*). Phylogeny of the North American scorpion genus *Diplocentrus* Peters, 1861 (Scorpiones: Diplocentridae) based on morphology, nuclear and mitochondrial DNA. *Arthropod Systematics & Phylogeny* **72**, 257–279.

Santibáñez-López, C. E., Francke, O. F., and Prendini, L. (2014*b*). *Kolotl*, n. gen. (Scorpiones: Diplocentridae), a new scorpion genus from Mexico. *American Museum Novitates* **3815**, 1–14. doi:10.1206/3815.1

Schliep, K. P. (2011). phangorn: phylogenetic analysis in R. *Bioinformatics* **27**, 592–593. doi:10.1093/bioinformatics/btq706

Sharma, P. P., Fernández, R., Esposito, L. A., González-Santillán, E., and Monod, L. (2015). Phylogenomic resolution of scorpions reveals multilevel discordance with morphological phylogenetic signal. *Proceedings of the Royal Society B* **282**, 20142953. doi:10.1098/rspb.2014.2953

Sissom, W. D. (1994). Descriptions of new and poorly known scorpions of Yemen (Scorpiones: Buthidae, Diplocentridae, Scorpionidae). *Fauna of Saudi Arabia* **14**, 3–39.

Stamatakis, A. (2014). RAxML version 8: a tool for phylogenetic analysis and post-analysis of large phylogenies. *Bioinformatics* **30**, 1312–1313. doi:10.1093/bioinformatics/btu033

Volschenk, E. S., and Prendini, L. (2008). *Aops oncodactylus*, gen. et sp. nov., the first troglobitic urodacid (Urodacidae: Scorpiones), with a re-assessment of cavernicolous, troglobitic and troglomorphic scorpions. *Invertebrate Systematics* **22**, 235–257. doi:10.1071/IS06054

Vrancken, B., Lemey, P., Rambaut, A., Bedford, T., Longdon, B., Günthard, H. F., and Suchard, M. A. (2015). Simultaneously estimating evolutionary history and repeated traits phylogenetic signal: applications to viral and host phenotypic evolution. *Methods in Ecology and Evolution* **6**, 67–82. doi:10.1111/2041-210X.12293

Handling editor: Gonzalo Giribet